GEOPHYSICAL RESEARCH LETTERS, VOL. 25, NO.15, PAGES 2971-2974, AUGUST 1, 1998

Effect of wave-particle interactions on ring current evolution for January 10-11, 1997: Initial results

V. K. Jordanova,[1] C. J. Farrugia,[1] J. M. Quinn,[1] R. M. Thorne,[2]
K. W. Ogilvie,[3] R. P. Lepping,[3] G. Lu,[4] A. J. Lazarus,[5]
M. F. Thomsen,[6] and R. D. Belian[6]

Abstract. We simulate the ring current evolution during the magnetic storm caused by Earth passage of the January 1997 magnetic cloud. Compared to previous studies, we include for the first time energy diffusion caused by wave-particle interactions. The modeled *Dst* index agrees reasonably well with the measured one, corrected for magnetopause currents and currents induced in the solid Earth. We compare H^+ distributions calculated from our model with those measured by the HYDRA instrument on the POLAR spacecraft and find that: a) the agreement between theory and data at large L shells ($L>5.5$) is very good; b) although the agreement at low L shells is improved when scattering by EMIC waves is included, the result is not entirely satisfactory, suggesting that either transport in a more realistic magnetospheric electric field or additional loss processes should be considered.

1. Introduction

Understanding the effect of plasma wave resonance on ring current evolution is an important issue in storm studies. Losses due to charge exchange and Coulomb collisions cannot fully explain the observed ring current decay [e.g., *Chen et al.*, 1998; *Jordanova et al.*, 1998]. Previous studies considering only pitch angle scattering caused by plasma waves have found that this effect can make a contribution of ~7% to the ring current energy loss during a major storm [*Kozyra et al.*, 1997] and of ~1-2% during a moderate storm [*Jordanova et al.*, 1997]. *Fok et al.* [1995, 1996] found that without the inclusion of wave scattering the ion fluxes at energies above a few tens of keV are too high and the calculated ion pitch angle distributions are too flat in comparison with observations during storm recovery.

In this study, we simulate the ring current evolution associated with the January 10-11, 1997 magnetic cloud passage, since an abundance of data pertinent to our modeling work is available from various ISTP spacecraft. We focus on the effect of wave-particle interactions by extending the model of *Jordanova et al.* [1997] to incorporate for the first time energy diffusion caused by plasma wave scattering. The model results are then compared with measurements from the HYDRA instrument on the POLAR spacecraft.

2. Interplanetary observations

The passage at Earth of the January 10-11, 1997 magnetic cloud caused a geomagnetic storm of moderate intensity with *Dst* reaching −85 nT. Interplanetary data on this magnetic cloud are shown in detail in Figures 1b and 2b of *Farrugia et al.* [1997]. An interplanetary shock is observed by WIND at ~hour 25 (Fig. 1a). In the magnetic cloud interval from ~hour 29 to ~hour 51, the magnetic field executes a large rotation, going from a south-easterly to a due northward orientation. The early $B_z<0$ phase lasts up to ~hour 41.5, followed by a generally $B_z>0$ interval lasting till the end of cloud passage. At the rear of the cloud, a high density plug is

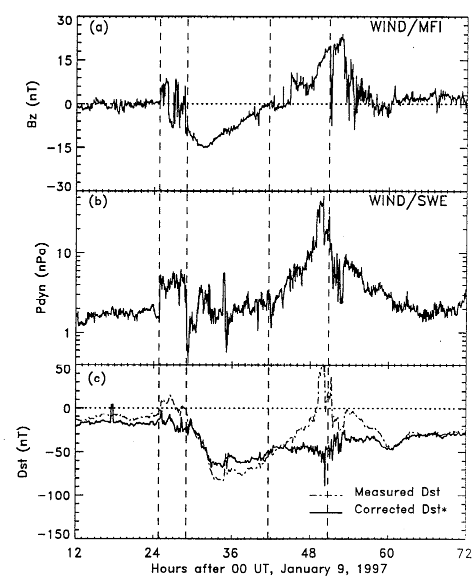

Figure 1. a) The north-south component of the IMF, B_z; b) Solar wind dynamic pressure; c) *Dst* index. The vertical lines show the shock; the cloud front boundary; the B_z transition inside the cloud; and the cloud rear boundary.

[1]SSC, University of New Hampshire, Durham.
[2]Department of Atmospheric Sciences, UCLA.
[3]NASA/GSFC, Greenbelt, Maryland.
[4]High Altitude Observatory, NCAR, Boulder, Colorado.
[5]Center for Space Research, MIT, Cambridge.
[6]LANL, Los Alamos, New Mexico.

Paper number 98GL00649.
0094-8534/98/98GL-00649$05.00

observed at WIND, which is thought to be prominence material [*Burlaga et al.*, 1998].

Figure 1b shows the dynamic pressure from measurements by the SWE instrument on WIND. As noted by *Farrugia et al.* [1997], the dynamic pressure varies over more than 2 orders of magnitude, being at its lowest (<0.5 nPa) just after cloud arrival, and at its highest (>40 nPa) during the high density plug. Around the density plug however there is increased dynamic pressure due to compression of the cloud's plasma and field by a fast corotating stream overtaking the cloud.

The 18-station measured (dashed-dotted line) and corrected (solid line) *Dst* are shown in Fig. 1c. Corrections for disturbed and quiet magnetopause currents, as well as currents induced in the solid Earth are included. Since the *Dst* data are 5 minute averages, appropriate propagation delays from WIND to ground have been taken into account when making these corrections. The main phase of the storm starts on cloud arrival. Moderately strong and constant activity persists during the "second" part of cloud passage (hour 42 - 51), but is attenuated after the rear of the cloud passes Earth.

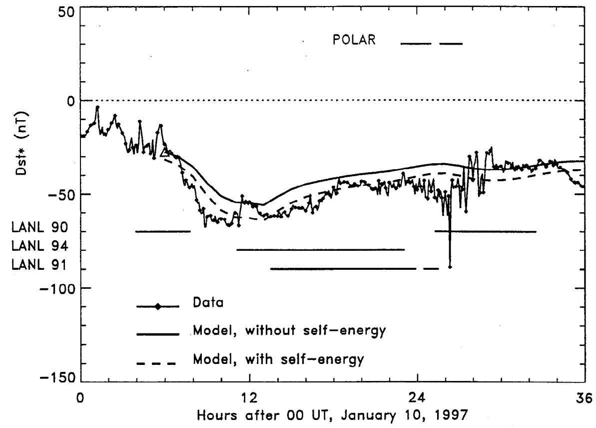

Figure 2. Comparison of model results (solid and dashed lines, as explained in legend) with the corrected *Dst* values (diamonds). The periods when POLAR was between L=2 and L=6.5 and LANL spacecraft were between MLT=18 and MLT=6 are indicated by horizontal lines.

3. Wave-particle interactions

The ring current evolution during the January 1997 magnetic storm is studied using our drift-loss model [*Jordanova et al.*, 1997]. The motion of energetic H^+ and O^+ ions in a time-varying Volland-Stern electric field and a 3D dipolar geomagnetic field is considered. Losses due to charge exchange, Coulomb collisions, plasma wave scattering and absorption of ring current ions at low altitude are included. The bounce-averaged kinetic equation for the phase space distribution F is solved as a function of time, t; equatorial radial distance, R_o; magnetic local time (MLT); kinetic energy of the particle, E; and $\mu_o = cos\alpha_o$, where α_o is the equatorial pitch angle. In previous studies, only the predominant plasma wave scattering mechanism, i.e., pitch angle diffusion, was considered. The addition to our model of energy diffusion caused by wave-particle interactions is discussed further below.

From quasi-linear theory, after transforming in (μ_o, E) variables and averaging between the mirror points, the energy diffusion term becomes:

$$\langle(\frac{\partial F}{\partial t})_{EE}\rangle = \frac{1}{\sqrt{E}}\frac{\partial}{\partial E}[\sqrt{E}\langle D_{EE}\rangle\frac{\partial F}{\partial E}] \qquad (1)$$

where

$$\langle D_{EE}\rangle = \frac{2mE}{h(\mu_o)}\int_0^{\lambda_m}\frac{D_{vv}}{\mu}\frac{(1-\mu^2)}{(1-\mu_o^2)}cos^7\lambda d\lambda. \qquad (2)$$

Here $h(\mu_o) = S_B/2R_o$, S_B is the half-bounce path length; m is the mass of the resonating particle; and λ_m is the magnetic latitude of the mirror point. We consider interactions with electromagnetic ion cyclotron (EMIC) waves and use the diffusion coefficients D_{vv} for particles resonating in a multicomponent plasma [*Jordanova et al.*, 1996]. The wave growth rates are obtained from the hot plasma dispersion relation, modeling the distribution of each ring current ion species (at each equatorial location) by a single bi-Maxwellian. Only the energy range from 1 keV up to 40 keV is fitted as this is the most unstable population [*Anderson et al.*, 1996]. We found that the convective growth rate maximizes for parallel propagating proton cyclotron waves from the He^+ wave branch (between the O^+ and He^+ gyrofrequencies), consistent with their observation mainly at low L near dusk [*Anderson et al.*, 1992]. Thus waves at lower and higher frequencies are excluded from this study. The effect of the wave-particle interactions on the ring current H^+ population is addressed. For this preliminary study, the ring current O^+ population evolves only through transport and collisional losses.

For the initial H^+ and O^+ ring current ion populations we use the statistical data set constructed from measurements by the CHEM spectrometer on the AMPTE/CCE satellite [*Kistler et al.*, 1989; *Jordanova et al.*, 1997]. The particle injection from the magnetotail is modeled using spin averaged fluxes measured by the MPA and SOPA instruments on the LANL geosynchronous satellites. The nightside coverage by the LANL satellites 90, 91, and 94 is shown in Fig. 2 (horizontal bars). When there are gaps in the data, we interpolate linearly.

4. Ring current evolution

The ring current contribution to the *Dst* index is obtained, based on the Dessler-Parker-Sckopke relation. We first modeled the ring current evolution during the January 10-11, 1997 storm period considering only losses due to charge exchange, Coulomb collisions, and ion absorption at low altitude in the atmosphere. The result is shown in Fig. 2 by the solid line, superimposed on the corrected *Dst* (diamonds). The model underestimates the rapidity of storm growth and the maximum strength of the storm. The dashed curve represents model results when the self energy of the ring current magnetic field is taken into account, assuming a nonlinearity parameter $\epsilon = 0.3$ [*Carovillano and Siscoe*, 1973]. The agreement between model and data is now improved. The largest remaining discrepancies occur a) during the rapid growth of the main phase and b) during the arrival of the high density plug (~hour 28). The first period coincided with a gap in the geostationary nightside coverage and we might have underestimated the plasma sheet density. As regards the latter, magnetospheric conditions were highly variable which makes the convection pattern strongly time-dependent on time scales that the Volland-Stern model (parameterized with the Kp index) cannot follow.

Wave-particle interactions are introduced into the model by calculating the equatorial convective growth rate of EMIC waves. The net wave gain is integrated along field-aligned wave paths extending over ±5° magnetic latitude (MLAT) to identify regions of maximum wave amplification. Previous studies have indicated the role of the plasmapause density gradient for keeping the wave normal angle field-aligned along an extended wave path and thus increasing the path-integrated gain [*Thorne and Horne*, 1992, 1997; *Kozyra et al.*, 1997]. We follow these works and consider an extended ±10° (±7.5°) wave path at the plasmapause (0.25 R_E wide on either side). We calculate an integrated wave gain, G, of up to ~35 dB during this period of moderate storm activity. These values are in agreement with those reported by *Hu and Fraser* [1994] for amplification of the He^+ branch waves generated inside the plasmasphere and with our previous study of wave generation during a moderate storm [*Jordanova et al.*, 1997]. Larger wave gain occurs during more active periods [*Kozyra et al.*, 1997] or at larger L values [*Horne and Thorne*, 1997]. Observations with the AMPTE/CCE spacecraft indicate that wave amplitudes in the inner magnetosphere are ~1–3 nT and could increase up to 10 nT [*Anderson et al.*, 1992; *Kozyra et al.*, 1997]. Since information on the background noise level which is amplified to produce observable waves is not available, the wave gain cannot be converted directly to wave amplitudes. *Thorne and Horne* [1997] suggest that 30 dB of wave gain are necessary to allow waves to grow to observable levels. In this preliminary work, we adopt a weaker criterion in order to study the potential effect of wave scattering on ring current evolution, and relate integrated wave gain with observed wave amplitudes through $B_w = 5\times10^{(G-25)/40}$

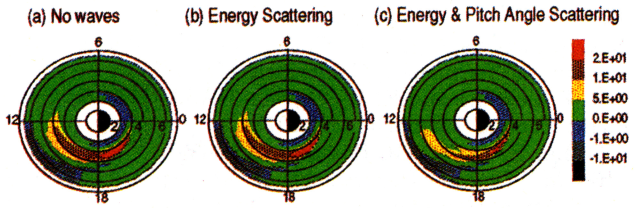

Figure 3. Calculated wave gain (dB) as a function of radial distance in the equatorial plane and MLT considering different loss processes (see text).

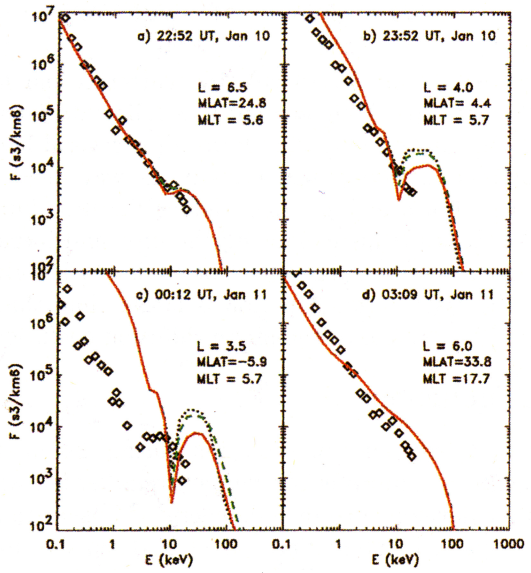

Figure 4. Measured HYDRA distributions (diamonds) compared with modeled distributions, considering only drift and collisional losses (black dotted line), and adding plasma wave-induced energy diffusion (green dashed line), and adding plasma wave-induced pitch angle scattering (red line).

nT. Where G>25, the wave amplitude is assumed to be 5 nT. The waves are neglected if $G\leq5$.

We found that stronger wave growth occurs after intensification of the ring current, i.e., Dst minimum, and lasts for several hours. The wave gain obtained at 12 UT, Jan. 10 when convection and all losses but plasma wave scattering are considered is shown in Fig. 3a; and adding plasma wave-induced energy diffusion in Fig. 3b; and adding plasma wave-induced pitch angle diffusion in Fig. 3c. In agreement with previous studies, the unstable regions are located in the postnoon to midnight sector near the region of enhanced thermal density just inside the plasmapause. Energy diffusion does not influence the calculated wave growth noticeably (Fig. 3a,b). Pitch angle diffusion, though, reduces the anisotropy of the proton population and further wave growth (Fig. 3c).

The bounce-averaged approach allows us to calculate the ring current distribution for different MLAT and to compare with off-equatorial POLAR data. The H^+ distribution function obtained with our model (solid line) and measurements (diamonds) from the HYDRA instrument [*Scudder et al.*, 1995] are shown in Fig. 4. For this period, HYDRA covered the energy range from 2 eV to 20 keV. Values of the locally mirroring (α=75°±15°) distribution functions are compared. The agreement between model and data is better at large L (6–6.5) than at low L (3.5–4). We now consider Fig. 4b,c, which refer to dawn. The unstable regions in our model are predominantly at dusk between L=3–4 (see Fig. 3). Calculations show that energy diffusion smoothes the spectrum, causing the distribution function F to decrease at energies from ~8 keV to ~50 keV within the unstable regions at dusk and to increase at higher energies. Pitch angle diffusion reduces the magnitude of F at $E \geq 8$ keV by scattering particles into the loss cone. Ring current ions follow drift paths around the Earth and reach dawn after several hours. The combined effects of scattering in the wave field and transport, shown in Fig. 4b,c, reduce the distribution at mid-energies (thus enhancing the dip) and increase it at higher energies. The effect of pitch angle scattering on the distribution function is larger than that of energy diffusion due to the larger diffusion coefficients.

5. Conclusions

We study ring current evolution during the January 10-11, 1997 storm using our ring current model, which is further developed to include energy diffusion caused by wave-particle interactions. The modeled Dst index compares reasonably well with the observed Dst when the latter is corrected for magnetopause currents and currents induced in the solid Earth. According to the calculated path-integrated gain of the amplified EMIC waves, the unstable regions are located just inside the plasmapause, in agreement with previous work. The effect of wave-particle interactions on the H^+ distribution is small and did not change the calculated Dst values significantly. The H^+ distribution function obtained from our model is compared with HYDRA data, showing a very good agreement at large L values. Although the disagreement at low L is reduced when resonance with proton cyclotron waves is considered, the result is not completely satisfactory. This suggests that convection in more realistic magnetic and electric fields, as well as resonance with other plasma waves, should be considered. We note that whereas pitch angle diffusion by proton cyclotron waves removes high energy particles by scattering them into the loss cone, thus contributing to the ring current energy loss, energy diffusion will partially compensate these losses by smoothing the energy spectra and increasing the high-energy population. Both processes should be considered when the effect of plasma wave resonance on the global energy balance of the ring current is addressed, especially during major storms when this effect is more important. Since the magnitude of the energy loss due to wave-particle interactions depends strongly on the assumed wave amplitudes, a comparative study of predicted wave gain with experimentally observed wave amplitudes will be performed in future to quantify this effect.

Acknowledgments. The decade-long efforts of the HYDRA hardware groups at NASA GSFC, UNH, Max Planck Lindau, and UCSD led by Jack Scudder, Roy Torbert, Axel Korth and Walker Fillius are gratefully acknowledged. This research is supported in part by NASA grants NAG 5 2231 and NAG 5 2834 and DARA grant 50 OC 8911 0. The work at UCLA is supported by NASA grant NAG 5 4680.

References

Anderson, B. J., et al., A statistical study of Pc 1-2 magnetic pulsations in the equatorial magnetosphere, 2. Wave properties, *J. Geophys. Res., 97*, 3089, 1992.

Anderson, B. J., et al., Observational test of local proton cyclotron instability in the Earth's magnetosphere, *J. Geophys. Res., 101*, 21527, 1996.

Burlaga, L. F., et al., A magnetic cloud containing prominence material: January 1997, *J. Geophys. Res., 103*, 277, 1998.

Carovillano, R. L., and G. L. Siscoe, Energy and momentum theorems in magnetospheric processes, *Rev. Geophys., 11*, 289, 1973.

Chen, M. W., et al., Simulations of ring current proton pitch angle distributions, *J. Geophys. Res., 165*, 1998.

Farrugia, C. J., et al., Geoeffectiveness of three WIND magnetic clouds: A comparative study, submitted to *J. Geophys. Res.*, 1997.

Fok, M.-C., et al., Three-dimensional ring current decay model, *J. Geophys. Res., 100*, 9619, 1995.

Fok, M.-C., et al., Ring current development during storm main phase, *J. Geophys. Res., 101*, 15311, 1996.

Horne, R. B., and R. M. Thorne, Wave heating of He^+ by electromagnetic ion cyclotron waves in the magnetosphere: Heating near the H^+-He^+ bi-ion resonance frequency, *J. Geophys. Res., 102*, 11457, 1997.

Hu, Y. D., and B. J. Fraser, Electromagnetic ion cyclotron wave amplification and source regions in the magnetosphere, *J. Geophys. Res., 99*, 263, 1994.

Jordanova, V. K., et al., Effects of heavy ions on the quasi-linear diffusion coefficients from resonant interactions with EMIC waves, *J. Geophys. Res., 101*, 19771, 1996.

Jordanova, V. K., et al., Kinetic model of the ring current-atmosphere interactions, *J. Geophys. Res., 102*, 14279, 1997.

Jordanova, V. K., et al., October 1995 magnetic cloud and accompanying storm activity: Ring current evolution, *J. Geophys. Res., 79*, 1998.

Kistler L. M., et al., Energy spectra of the major ion species in the ring current during geomagnetic storms, *J. Geophys. Res., 94*, 3579, 1989.

Kozyra, J. U., et al., Modeling of the contribution of electromagnetic ion cyclotron (EMIC) waves to stormtime ring current erosion, in *Magnetic Storms, Geophys. Monogr. Ser.*, vol. 98, edited by B. T. Tsurutani, W. D. Gonzalez, and Y. Kamide, p. 187, AGU, Washington, D. C., 1997.

Scudder, J., et al., HYDRA - A 3-dimensional electron and ion hot plasma instrument for the POLAR spacecraft of the GGS mission, *Space Sci. Rev., 71*, 459, 1995.

Thorne, R. M., and R. B. Horne, The contribution of ion-cyclotron waves to electron heating and SAR-arc excitation near the storm-time plasmapause, *Geophys. Res. Lett., 19*, 417, 1992.

Thorne, R. M., and R. B. Horne, Modulation of electromagnetic ion cyclotron instability due to interaction with ring current O^+ during magnetic storms, *J. Geophys. Res., 102*, 14155, 1997.

R. D. Belian and M. F. Thomsen, Los Alamos National Laboratory, Los Alamos, NM 87545.

C. J. Farrugia, V. K. Jordanova, and J. M. Quinn, Space Science Center, University of New Hampshire, Durham, NH 03824. (e-mail: vania.jordanova@unh.edu)

A. J. Lazarus, Center for Space Research, Massachusetts Institute of Technology, Cambridge, MA 02139.

R. P. Lepping and K. W. Ogilvie, NASA Goddard Space Flight Center, Greenbelt, MD 20771.

G. Lu, HAO, NCAR, Boulder, CO 80307.

R. M. Thorne, Department of Atmospheric Sciences, University of California, Los Angeles, CA 90095.

(Received October 14, 1997; revised January 19, 1998; accepted February 9, 1998.)